JOURNAL OF NANO- AND ELECTRONIC PHYSICS
Vol. 17 No 1, 01012(6pp) (2025)

ЖУРНАЛ НАНО- ТА ЕЛЕКТРОННОЇ ФІЗИКИ
Том 17 № 1, 01012(6cc) (2025)

REGULAR ARTICLE

Modeling of Surface-Emitting Terahertz Quantum Cascade Laser Based on Difference Frequency Generation

A. Hamadou[1,2,*], J.-Luc. Thobel[3,†]

[1] Département d'Optique, Institut d'Optique et de Mécanique de Précision, Université Sétif 1, 19000 Algeria
[2] Laboratoire D'étude des Surfaces et Interfaces des Matériaux Solides (LESIMS), Université Sétif 1, 19000 Algeria
[3] Institut d'Electronique, de Microélectronique et de Nanotechnologie (IEMN), UMR 8520, Université Lille 1, Avenue Poincaré, BP 60069, 59652 Villeneuve d'Ascq Cédex, France

(Received 25 December 2024; revised manuscript received 18 February 2025; published online 27 February 2025)

In this paper, we propose a simple method to calculate the THz field and THz power generated via intracavity difference frequency generation in a dual-wavelength mid-infrared quantum cascade laser. The approach is based on using a surface emission scheme in the nonlinear waveguide. The results show that the THz output power varies linearly with the product of the tow mid-infrared pump powers, and strongly depends on the cover refractive index for the THz waves. Specifically, a higher refractive index leads to a significant increase in THz power, while a low product of the pump powers levels result in weak output power. Additionally, the effect of nonlinear film thickness on optical efficiency is considered. The efficiency decreases as the film thickness increases. This is due to the dependence of the THz field amplitude in the cover region on the film-substrate and film-cover interfaces, which is significantly affected by the film thickness. Our model generates output power through surface emission, in agreement with existing experimental results, highlighting the importance of optimizing the cover material and film thickness to improve output power and THz efficiency.

Keywords: Terahertz quantum cascade laser, Difference-frequency generation, Surface emission scheme, Optical efficiency.

DOI: 10.21272/jnep.17(1).01012 PACS numbers: 42.55.Ah, 42.55.Px

1. INTRODUCTION

The terahertz wave (THz-wave) generation technique has garnered significant interest recently due to its remarkable potential applications in field such as imaging, spectroscopy, communications, security, and nondestructive testing [1, 2]. Just a few years after the initial demonstration of THz waves in quantum cascade (QC) laser [3-5], a THz source based on intracavity difference frequency generation (DFG) in dual-wavelength mid-infrared (mid-IR) QC laser with giant second-order nonlinear susceptibility was developed [6, 7]. Unfortunately, the significant free carrier absorption of the device in the THz range (measured at 250 cm^{-1} at 80 μm [8]) means that the THz radiation generated in the optical waveguide can be subsequently absorbed. For example, the commonly employed bound-to-continuum and double phonon resonance scheme has a conversion efficiency of 250 μW/W^2 at 3.8 THz [6]. However, it took an additional 16 years to enhance the extremely low conversion efficiencies by introducing the concept of surface-emitting DFG based on second-order nonlinear susceptibility in the active region of the QC laser [9-11]. The surface-to-facet THz emission ratio was improved and is within the range of 2-5 for several devices [9].

In the surface-emitting configuration of DFG, THz radiation is extracted vertically from the whole length of the waveguide. This geometry can be utilized to reduce the absorption loss of THz waves in nonlinear materials. Second-order grating-couplers can be used to extract THz radiation from the waveguide. The initial structure of this scheme consists of an active region composed of two stacks of stages. The first stack features a double phonon resonance design [12] with lasing occurring at a wavelength of $\lambda_1 = 10.5$ μm. In contrast, the second stack employs a bound-to-continuum design [12] with lasing taking place at a wavelength λ_2 approximately 8.9 μm. To obtain more detailed technical information about the structure used here we kindly refer the reader to the published literature [7, 13, 14]. In this paper, we develop a simple theoretical model to calculate the THz power generated via intracavity difference frequency in nonlinear waveguide utilizing the surface emission scheme.

2. THEORY

2.1 Derivation of the THz Mode of the Waveguide

Fig. 1 illustrates the schematic representation of surface-emitted DFG for wave generation in a planar optical waveguide that we are discussing. We consider two

* Correspondence e-mail: abd_hamado@yahoo.fr
† Jean-Luc.Thobel@laposte.net

Cite this article as: A. Hamadou et al., *J. Nano- Electron. Phys.* 17 No 1, 01012 (2025) https://doi.org/10.21272/jnep.17(1).01012

QC lasers in the lowest order TM mode with frequencies ω_1 and ω_2 corresponding to a double phonon resonance design and a bound-to-continuum design, respectively. These two QC lasers propagate into a nonlinear planar film made of InGaAs/InAlAs. The film is characterized by refractive indices n_{1f} and n_{2f} and a susceptibility $\chi^{(2)}$. The nonlinear film is located between two regions: a cover layer with refractive indices n_{1c} and n_{2c} and a substrate layer with refractive indices n_{1s} and n_{2s}. The THz wave generated through DFG is emitted in a direction perpendicular to the waveguide. The period of the second-order grating is denoted by Λ. Note that the two mid-IR QC lasers are used here as pumps sources to generate THz frequency via the DFG process within the film.

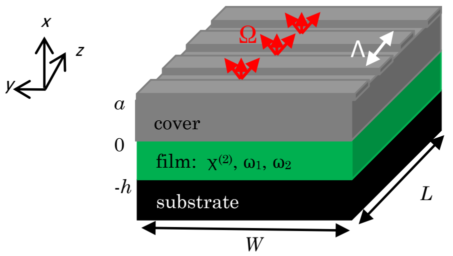

Fig. 1 – The scheme of surface-emitted DFG for THz wave generation in planar optical waveguide. The nonlinear active region is shown in green. Red solid arrows indicate the terahertz radiation emission at an angle from the surface

The fundamental magnetic fields of the TM mode, $\mathcal{H}_{1y}$ and $\mathcal{H}_{2y}$, in the cover, film, and substrate regions can be expressed as [15]

$$\mathcal{H}_{jy}(x)=\begin{cases}-C_j\dfrac{n_{jc}^2}{n_{jf}^2}\dfrac{q_{jf}}{q_{jc}}\exp(-q_{jc}x), & (1a)\\[2ex] -C_j\left(\dfrac{n_{jc}^2}{n_{jf}^2}\dfrac{q_{jf}}{q_{jc}}\cos(q_{jf}x)+\sin(q_{jf}x)\right)\exp(q_{js}(x+h)), & (1b)\\[2ex] C_j\left(-\dfrac{n_{jc}^2}{n_{jf}^2}\dfrac{q_{jf}}{q_{jc}}\cos(q_{jf}x)+\sin(q_{jf}x)\right), & (1c)\end{cases}$$

where the subscript j denotes either 1 or 2, and the three parameters for the two mid-IR pumps are defined as [15] $q_{jc}^2=\beta_j^2-k_j^2n_{jc}^2$, $q_{jf}^2=k_j^2n_{jf}^2-\beta_j^2$, and $q_{js}^2=\beta_j^2-k_j^2n_{js}^2$, with $k_j=\omega_j/c$ where c is the speed of light in vacuum. The propagation constant β_j for both confined mid-IR pumps are solutions to the equation in Ref. [15], derived for one mode, while C_j is the amplitude coefficient for the two mid-IR pumps and can be expressed as [15]

$$C_j=\sqrt{\frac{4\omega_j\varepsilon_0P_j}{W\beta_jh_{eff,j}}}, \qquad (2)$$

where $P_j\,(j=1,2)$ represents the mid-IR pumps power at frequency ω_j, and $h_{eff,j}$ corresponds to the effective depth for the TM mode at that frequency, as described in Ref. [15], derived for a single mode.

Our computation uses the following QC laser parameters at T = 80 K as reported in Refs. 6 and 9: $n_{1s}\approx n_{2s}\approx 3.11$, $n_{1f}\approx 3.176$, $n_{2f}\approx 3.19$, $n_{1c}\approx n_{2c}\approx 3$, $\lambda_1=10.5\ \mu\text{m}$, $\lambda_2=8.9\ \mu\text{m}$, L = 2 mm, W = 24 μm, $\chi^{(2)}=4\times10^4$ pm/V.

We now proceed to calculate the THz field to establish the THz power coupled perpendicularly to the waveguide. The THz magnetic field distribution $H_{THz,y}(x)$ is the solution to the wave equation in the film, given by

$$\frac{\partial^2H_{THz,y}}{\partial x^2}+\frac{\partial^2H_{THz,y}}{\partial y^2}-\left(\frac{n_{THz,f}}{c}\right)^2\frac{\partial^2H_{THz,y}}{\partial t^2}=\sqrt{\varepsilon_0\mu_0}\,\frac{\partial^2P_{THz}^{(2)}}{\partial t^2}, \qquad (3a)$$

and in the substrate and cover waveguide, expressed as

$$\frac{\partial^2H_{THz,y}}{\partial x^2}+\frac{\partial^2H_{THz,y}}{\partial y^2}-\left(\frac{n_{THz,i}}{c}\right)^2\frac{\partial^2H_{THz,y}}{\partial t^2}=0,\ i=s,c \qquad (3b)$$

respectively. In the above equations μ_0 is the permeability in vacuum, $n_{THz,f}$ and $n_{THz,i}$ are the respective refractive indices in the film, substrate ($i=s$), and cover ($i=c$) waveguides at the DFG frequency, $P_{THz}^{(2)}$ represents the terahertz radiation generated by the nonlinear polarization induced by the two mid-IR pumps in the QC laser active region with nonlinear susceptibility $\chi^{(2)}$ and can be expressed as [9]

$$P_{THz}^{(2)}(z,t)=\varepsilon_0\chi^{(2)}E_{1x}E_{2x}^*\exp\left[i(\beta_sz-\Omega t)\right], \qquad (4)$$

where $\Omega=\omega_1-\omega_2$ represents the DFG frequency and $\beta_s=\beta_1-\beta_2$ denotes the propagation constant, while E_{1x} and E_{2x}^* are the x-components of the mode profiles of the mid-IR guided waves at ω_1 and ω_2. The electric fields component E_{1x} and E_{2x}^* can be expressed in terms of the fundamental magnetic fields components of the TM mode, $\mathcal{H}_{1y}$ and $\mathcal{H}_{2y}^*$, as derived in [15] for one mode.

The y-component of the magnetic THz-wave $H_{THz,y}(x,z,t)$ can be separated into the following form

$$H_{THz,y}(x,z,t)=\mathcal{H}_{THz,y}(x)\exp\left[i(\beta_sz-\Omega t)\right], \qquad (5)$$

where $\mathcal{H}_{THz,y}$ is the slowly varying envelope of the magnetic field distribution function.

By substituting $\partial/\partial y=0$ into Eq.(3) and considering Eq. (5), the wave equations (3) for the cover, film, and substrate regions, respectively, can be expressed as follows:

$$\frac{\partial^2\mathcal{H}_{THz,y}}{dx^2}+\left(\frac{\Omega^2n_{THz,c}^2}{c^2}-\beta_s^2\right)\mathcal{H}_{THz,y}(x)=0, \qquad (6a)$$

$$\frac{\partial^2 \mathscr{H}_{THz,y}}{dx^2}+\left(\frac{\Omega^2 n_{THz,f}^2}{c^2}-\beta_s^2\right)\mathscr{H}_{THz,y}(x)= \\ =-\sqrt{\varepsilon_0\mu_0}\,\Omega^2\varepsilon_0\chi^{(2)}E_{1x}E_{2x}^*(x) \quad (6b)$$

$$\frac{\partial^2 \mathscr{H}_{THz,y}}{dx^2}+\left(\frac{\Omega^2 n_{THz,s}^2}{c^2}-\beta_s^2\right)\mathscr{H}_{THz,y}(x)=0\,. \quad (6c)$$

Here, we assume that the refractive indices of the waveguide cover, film and substrate are the same at the difference frequency.

The y-component $\mathscr{H}_{THz,y}$ of the terahertz mode, the solution of equations (6), is described by the following expressions for the cover, film, and substrate regions, respectively

$$\mathscr{H}_{THz,y}(x)=\begin{cases} De^{ik_c x}\,, & (7a)\\ Ae^{-ik_f(x+h)}+Be^{ik_f(x+h)}+QF_f(x)\,, & (7b)\\ Ce^{-ik_s(x+h)}\,, & (7c)\end{cases}$$

where $QF_f(x)$ in Eq. (7b) is a particular solution of Eq.(6b) that represents the forced field generated directly by the nonlinear polarization wave with $Q=k_0\chi^{(2)}C_1C_2$, while A, B, C, and D are constants and can be determined by the boundary conditions, and the parameters k_c, k_f, k_s, and $F_f(x)$ are related to the propagation constant by $k_c=\sqrt{k_0^2 n_{THz,c}^2-\beta_s^2}$, $k_f=\sqrt{k_0^2 n_{THz,f}^2-\beta_s^2}$, $k_s=\sqrt{k_0^2 n_{THz,s}^2-\beta_s^2}$, and

$$F_f(x)=\sqrt{\frac{\varepsilon_0}{\mu_0}}\frac{k_0}{2}\frac{\beta_1\beta_2}{\omega_1\omega_2\varepsilon_0^2 n_{THz,f}^4}\times \\ \times\sqrt{1+\left(\frac{n_{1c}^2}{n_{1f}^2}\frac{q_{1f}}{q_{1c}}\right)^2}\sqrt{1+\left(\frac{n_{2c}^2}{n_{2f}^2}\frac{q_{2f}}{q_{2c}}\right)^2}\Phi(x)\,, \quad (8a)$$

with $k_0=\Omega/c$ is the wavenumber at terahertz frequency and

$$\Phi(x)=\frac{\cos\left((q_{1c}+q_{2c})x+\varphi_1+\varphi_2\right)}{\left((q_{1c}+q_{2c})^2-k_f^2\right)}+ \\ +\frac{\cos\left((q_{1c}-q_{2c})x+\varphi_1-\varphi_2\right)}{\left((q_{1c}-q_{2c})^2-k_f^2\right)}\,, \quad (8b)$$

where the parameters φ_1 and φ_2 are defined as

$$\tan\varphi_j=\left(\frac{n_{jf}}{n_{jc}}\right)^2\frac{q_{jc}}{q_{jf}}\,. \qquad j=1,2 \quad (9)$$

According to Eq. (7), the coefficients A, B, C, and D can be obtained by applying the continuity conditions of $\mathscr{H}_{THz,y}$ and $d\mathscr{H}_{THz,y}/dx$ at the interfaces $x=0$ and $x=-h$. This yields the following expression for the field amplitude in the cover region:

$$|D|=Q\sqrt{D_1^2+D_2^2}\,, \quad (10)$$

where the parameters D_1 and D_2 indicate that the magnetic field in the cover region is governed by the boundary conditions at both the film-substrate and at the film-cover interfaces of the waveguide.

$$D_1=\frac{\frac{\partial F_f(0)}{\partial x}\sin(hk_f)-k_fF_f(0)\cos(hk_f)+k_fF_f(-h)}{k_c+k_f}\,, \quad (11a)$$

$$D_2=\frac{\frac{\partial F_f(0)}{\partial x}\cos(hk_f)-k_fF_f(0)\sin(hk_f)-\frac{\partial F_f(-h)}{\partial x}}{k_c+k_f}\,. \quad (11b)$$

2.2 Output Surface-Emitted Power

In the following analysis, we use the scalar diffraction theory. The far-field distribution $\mathscr{H}_{THz}(\theta,\varphi)$ in the directions θ and φ at distance R from a center of the grating is given by the Fresnel-Kirchhoff theory as a 2D integral [16]:

$$\mathscr{H}_{THz}(\theta,\varphi)=\frac{1}{\lambda R}\int_{-\frac{W}{2}}^{\frac{W}{2}}\int_{-\frac{L}{2}}^{\frac{L}{2}}\tau\mathscr{H}_{THz,y}(h,z,t)\frac{2}{\pi}\cos\left(\frac{2\pi}{\Lambda}z\right)\times \\ e^{ik_0(z\cos\theta+y\sin\theta\sin\varphi)}dzdy\,. \quad (12)$$

where λ represents the wavelength of THz field, τ denotes the Fresnel transmittance coefficient in the slots of the grating and given by $\tau=2k_c/(k_c+k_0)$, $\mathscr{H}_{THz,y}$ is the THz-magnetic-field distribution on the surface of the grating, θ is the angle formed between the direction of observation and the z-axis, while φ is the angle between the x-axis and the projection of vector R onto the (xy)-plane.

It follows that in Eq. (12), the variables z and y can be separated. The THz surface-emitted radiation distribution is then expressed as the product of two one-dimensional functions, which is equal to

$$\mathscr{H}_{THz}(\theta,\varphi)=\frac{\tau DWLe^{-i\Omega t}e^{ik_c a}}{\pi\lambda R}\times \\ \times\sin c\left(\frac{k_0W\sin\theta\sin\varphi}{2}\right)\times\sin c\times\left(\frac{k_0L\cos\theta}{2}\right), \quad (13)$$

where we use the expression for the magnetic field in the cover, and for $\Lambda=2\pi/\beta_s$, which is needed for the THz-wave surface emitted DFG. In the above equation, the function $\sin c(x)$ is defined as $\sin(x)/x$.

In order to get the surface-emitted THz power, it is convenient to determine the intensity of the THz-field in terms of QC laser parameters and the angular distributions θ and φ. The intensity of surface-emitted radiation is related to the electric field by $I_{THz}=n_{THz}E_{THz}E_{THz}^*/(2Z_0)$ where $Z_0=\sqrt{\mu_0/\varepsilon_0}$ is the free-space impedance. Using the expression for the magnetic field in the cover and applying the relationship between the magnetic and electric fields $|\mathscr{H}|=n_{THz}|E|/Z_0$ one gets:

$$
\begin{aligned}
I_{THz}(\theta,\varphi) = \frac{Z_0}{2n_{THz}} \times \left(\frac{\tau DWL}{\pi\lambda R}\right)^2 \times \\
\times \sin c^2\left(\frac{\pi W \sin\theta \sin\varphi}{\lambda}\right) \times \sin c^2 \times \left(\frac{\pi L \cos\theta}{\lambda}\right)
\end{aligned}, \quad (14)
$$

where $\frac{Z_0}{2n_{THz}}\left(\frac{\tau DWL}{\pi\lambda R}\right)^2$ is the intensity at the center of the grating. It is worth noting that the last two factors attain their maximum values at $\varphi = 0$ and $\theta = \pi/2$, respectively and therefore the maximum radiation occurs along the x-axis i.e., in the direction normal to the waveguide surface.

In Fig. 2, the normalized intensity is plotted as a function of the angle θ, for three values of the number of slits N. We observe that as N increases, the peak becomes narrower, and more light is concentrated in the central peak. Note that the main lobe of the $\sin c^2(x)$ function is very close to a Gaussian function with a standard deviation of $2\sqrt{\pi}$, i.e., $\Delta\theta \approx \lambda / \left(L\sqrt{2\pi\sqrt{\pi}}\right)$ and $\Delta\varphi \approx \lambda / \left(W\sqrt{2\pi\sqrt{\pi}}\right)$.

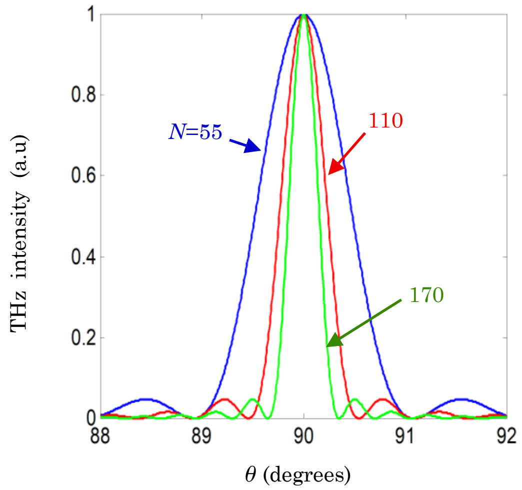

Fig. 2 – Intensity of N slits diffraction as a function of θ for three values of N where h = 3 μm

The power of the surface-emitted DFG radiation is related to the intensity by $P_{THz}^{surf} \approx I_{THz} R^2 \Delta\theta\Delta\varphi$. From Eq. (14), we obtain the expression for the total THz-radiated power out of the core

$$
P_{THz}^{surf} \approx \frac{1}{\sqrt{\pi}}\left(\frac{k_c}{k_c + k_0}\right)^2 \frac{Z_0 WL}{\pi^3 n_{THz}} |D|^2 . \quad (15)
$$

As we can see from Eq. (15), the surface-emitted THz power depends on the materials parameters of the QC laser and can be controlled either through the cover's refractive index for THz-wave or by the film thickness.

Fig.3 shows the variation of the surface-emitted output power with the product of two mid-IR pump powers for different cover refractive indices for THz wave, the results are obtained for a nonlinear film thickness of 3 μm. From this figure, it can be observed that the THz output power varies linearly with the product of two mid-IR pump powers and depends strongly on the cover refractive index. Moreover, a considerable increase in the THz output power is observed as the cover refractive index increases, as shown in this figure. Finally, when the product of the two mid-IR pump powers is small, the THz power is low. In Fig. 4, the surface-emitted THz power is plotted versus cover refractive index for three values of the product of the two mid-IR pump powers, and we can easily see that the THz power is an increasing function of both parameters. As a results, we conclusion that the waveguide cover material should have a high refractive index for terahertz waves.

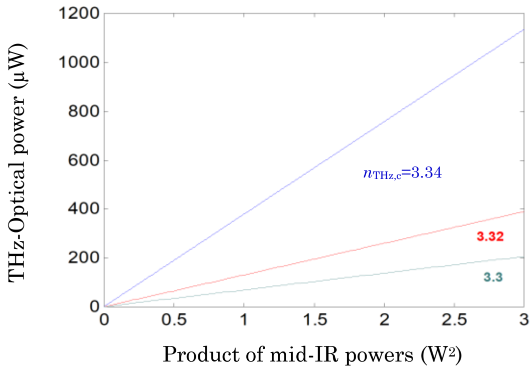

Fig. 3 – Variation of surface emitted THz-power versus product of two mid-IR pump powers for different cover refractive index for a THz-wave where h = 3 μm

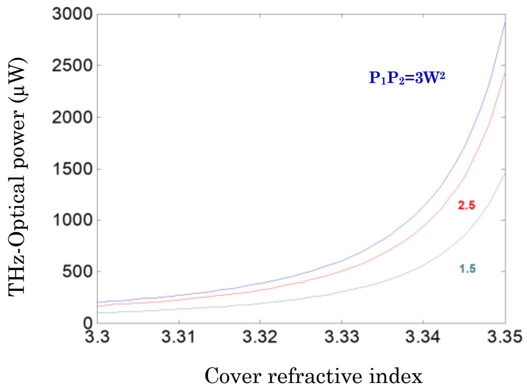

Fig. 4 – Variation of surface emitted THz-power versus cover refractive index for a THz-wave for different product of two mid-IR pump powers where h = 3 μm

We now want to derive a general expression for the optical efficiency per unit length η which is an important parameter that characterizes the optical performance of a surface-emitted THz QC laser. This quantity is defined as the ratio of the THz surface-emitted conversion efficiency due to DFG per unit length of the waveguide, i.e., $\eta = P_{THz}^{surf} / P_1 P_2 L$.

Fig.5 shows the variation of the optical efficiency per unit length η of the THz surface-emitted DFG with film thickness for different cover refractive indices for THz wave. As can be easily observed, the efficiency decreases significantly as the film thickness increases. The physical reason for this result is apparent: the power of the surface-emitted DFG depends strongly on the amplitude of THz field D in the cover region due to its dependence on the forced field at both the film-substrate and film-cover interfaces of the waveguide, and the latter depends significantly on the film thickness. We also observe that the efficiency depends on the value of $n_{THz,c}$.

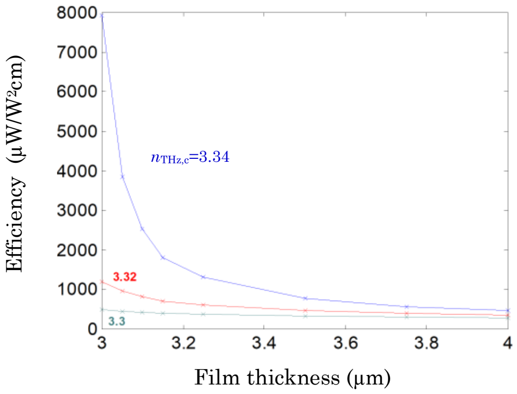

Fig. 5 – Dependence of optical efficiency η per unity length as a function of film thickness for three values of cover refractive index for a THz-wave

To conclude our analysis, we compare the THz powers emitted from the surface and the facet $G = P_{THz}^{surf} / P_{THz}^{facet}$, where P_{THz}^{facet} represents the phase-matched THz-DFG power derived from collinear geometry in QC laser waveguides, as indicated in [6], with absorption at the radiation wave frequency being taken into consideration

$$P_{THz}^{facet} = \frac{\Omega^2}{8\varepsilon_0 c^3 n_{1f} n_{2f} n_{THz}} \left|\chi^{(2)}\right|^2 \frac{P_1 P_2}{S_{eff}} \ell_{eff}^2 T_{THz} . \qquad (16)$$

Here, S_{eff} represents the effective area of interaction of the pump beams in the film, ℓ_{eff} is the effective length of the nonlinear interaction, and T_{THz} is the transparency coefficient at the THz frequency. Assuming $P_1P_2 = 3$ W², $n_{THz,c} \approx n_{THz,f}$, $T_{THz} \approx 0.15$, $S_{eff} \approx 4\times10^3$ μm², $\ell_{eff} \approx 80$ μm [6,8], this expression leads to a theoretical value of $G \approx 11$, 21 and 158 for $n_{THz,c} = 3.3$, 3.32 and 3.35 respectively.

3. CONCLUSIONS

In conclusion, we propose a surface-emitting THz wave source based on difference-frequency generation in a dual-wavelength mid-IR QC laser. Analytical expressions for the THz field and output power have been obtained. Using the current design and physical parameters, the film thickness and the cover refractive index for THz wave are found to play a central role in the performance of THz surface-emitted power. The agreement between our model and experimental data supports the validity of the proposed model. This approach offers a promising way to realize a miniaturized, easy-to-use, robust THz wave source.

ACKNOWLEDGMENTS

The authors are grateful to the Algerian Ministry of Higher Education for a research grant and to the Institut d'Electronique, de Microélectronique et de Nanotechnologie (IEMN), Lille1 France for his support.

REFERENCES

1. P.U. Jepsen, D.G. Cooke, M. Koch, *Laser Photon. Rev.* **5**, 124 (2011).
2. P. Dean, A. Valavanis, J. Keeley, K. Bertling, Y.L. Lim, R. Alhathlool, A.D. Burnett, L.H. Li, S.P. Khanna, D. Indjin, T. Taimre, A.D. Rakić, E.H. Linfield, A.G. Davies, *J. Phys. D: Appl. Phys.* **47**, 374008 (2014).
3. R. Köhler, A. Tredicucci, F. Beltram, H.E. Beere, E.H. Linfield, A.G. Davies, D.A. Ritchie, R.C. Iotti, F. Rossi, *Nature* **417**, 156 (2002).
4. G. Scalari, L. Ajili, J. Faist, H. Beere, E. Linfield, D. Ritchie, G. Davies, *Appl. Phys. Lett.* **82** No 19, 3165 (2003).
5. S. Kumar, C.W.I. Chan, Q. Hu, J.L. Reno, *Nat. Phys.* **7**, 166 (2011).
6. M.A. Belkin, F. Capasso, F. Xie, A. Belyanin, M. Fischer, A. Wittmann, J. Faist, *Appl. Phys. Lett.* **92**, 201101 (2008).
7. K. Vijayraghavan, R.W. Adams, A. Vizbaras, M. Jang, C. Grasse, G. Boehm, M.C. Amann, M.A. Belkin, *Appl. Phys. Lett.* **100** No 25, 251104 (2012).
8. R.-W. Adams, A. Vizbaras, M. Jang, C. Grasse, S. Katz, G. Boehm, M.-C. Amann, M.-A. Belkin, *Appl. Phys. Lett.* **98**, 151114 (2011).
9. C. Pflugl, M. A. Belkin, Q. J. Wang, M. Geiser, A. Belyanin, M. Fischer, A. Wittmann, J. Faist, F. Capasso, *Appl. Phys. Lett.* **93**, 161110 (2008).
10. F. Demmerle, W. Oberhausen, D. Burghart, A. Wolf, G. Kumar Veerabathran, J.-H. Krakofsky, H. Schmeiduch, G. Böhm, M.-C. Amann, *Opt. Eng.* **57** No 1, 011007 (2018).
11. J.-H. Kim, S. Jung, Y. Jiang, K. Fujita, M. Hitaka, A. Ito, T. Edamura, M.-A. Belkin, *Appl. Phys. Lett.* **113**, 161102 (2018).
12. J. Faist, D. Hofstetter, M. Beck, T. Aellen, M. Rochat, S. Blaser, *IEEE J. Quantum Electron.* **38** No 6, 533 (2002).
13. Q. Lu, M. Razeghi, *Photonics* **3** No 3, 42 (2016).
14. K. Fujita, S. Junga, Y. Jiang, J.-H. Kim, A. Nakanishi, A. Ito, M. Hitaka, T. Edamura, M.-A. Belkin, *Nanophotonics* **7** No 11, 1795 (2018).
15. H.-F. Taylor, A. Yariv, *Proc. IEEE* **62** No 8, 1044 (1974).
16. M. Born, E. Wolf, *Principles of Optics* (Macmillan: New York: 1964).

Моделювання терагерцового квантового каскадного лазера поверхневого випромінювання на основі генерації різної частоти

A. Hamadou[1,2], J.-Luc. Thobel[3]

[1] *Département d'Optique, Institut d'Optique et de Mécanique de Précision, Université Sétif 1, 19000 Algeria*
[2] *Laboratoire D'étude des Surfaces et Interfaces des Matériaux Solides (LESIMS), Université Sétif 1, 19000 Algeria*
[3] *Institut d'Electronique, de Microélectronique et de Nanotechnologie (IEMN), UMR 8520, Université Lille 1, Avenue Poincaré, BP 60069, 59652 Villeneuve d'Ascq Cédex, France*

У даній статті запропоновано простий метод обчислення ТГц поля та ТГц потужності, що генеруються за допомогою генерації різницевої частоти всередині резонатора в квантовому каскадному лазері середньої довжини хвилі інфрачервоного діапазону. Підхід заснований на використанні схеми поверхневого випромінювання в нелінійному хвилеводі. Результати показують, що вихідна потужність ТГц змінюється лінійно в залежності від добутку двох потужностей накачування в середньому інфрачервоному діапазоні та сильно залежить від показника заломлення покриття для хвиль ТГц. Зокрема, вищий показник заломлення призводить до значного збільшення потужності ТГц, тоді як низький добуток рівнів потужності накачування призводить до слабкої вихідної потужності. Додатково розглядається вплив нелінійної товщини плівки на оптичну ефективність. Зі збільшенням товщини плівки ефективність знижується. Це пов'язано із залежністю амплітуди ТГц поля в області покриття від межі розділу плівка-підкладка та плівка-покриття, на яку суттєво впливає товщина плівки. Представлена модель генерує вихідну потужність через поверхневе випромінювання відповідно до наявних експериментальних результатів, що підкреслює важливість оптимізації матеріалу покриття та товщини плівки для підвищення вихідної потужності та ефективності ТГц.

Ключові слова: Терагерцовий квантовий каскадний лазер, Генерація частоти, Схема поверхневого випромінювання, Оптична ефективність.